Precisely Correcting SMN Deficiency Pathways in Spinal Muscular Atrophy Using an Off-Amyloid Stabilizer

I-Fan Wang

ifanwang.gbs@gmail.com

Garage Brain Science

Chen-Hung Ting

Garage Brain Science

Li-Kai Tsai

Department of Neurology, National Taiwan University Hospital and National Taiwan University College of Medicine

Hsiang-Yu Chang

Garage Brain Science

Hsing-Jung Lai

Department of Neurology, National Taiwan University Hospital and National Taiwan University College of Medicine

Gunn-Guang Liou

Office of Research and Development, College of Medicine, National Taiwan University

Chien-Lin Chen

Department of Neurology, National Taiwan University Hospital and National Taiwan University College of Medicine

Article

Keywords: survival motor neuron (SMN) proteins, spinal muscular atrophy (SMA), prion-like low complexity (LC) domain, TDP-43 proteinopathies, gems and baicalein

Posted Date: July 11th, 2024

DOI: https://doi.org/10.21203/rs.3.rs-4586057/v1

Additional Declarations: Yes there is potential Competing Interest. H.-Y. Chang, C.-H. Ting and I.-F Wang are financially compensated as employees of Garage Brain Science Co., Ltd. in Taiwan and YEEFAN MED INC. in the US.

Abstract

While therapies like Spinraza, Zolgensma, and Evrysdi focus on increasing SMN1 protein levels to treat spinal muscular atrophy (SMA), their effectiveness is limited and highly dependent on early intervention. This indicates that merely augmenting SMN levels may not adequately reverse the permanent pathological effects stemming from SMN1 deficiency. Our research indicates that SMA is a protein conformational disorder rather than solely a splicing disease. We found that the SMN protein contains prion-like domains located in exon 2 and exons 6-7. Due to the absence of exon 7, the SMNΔ7 variant displays reduced prion-like activity. This deficit hampers gemins and RNPs formation and leading to persistent misfolded TDP-43 and PFN1 proteins despite treatment with Spinraza and Evrysdi. Remarkably, treatment with baicalein, a prion-like folding stabilizer, enabled SMNΔ7 to form a prion-like structure, restored the assembly of gemins and RNPs, effectively cleared toxic aggregated TDP-43 proteins and alleviated symptoms in SMA models.

Introduction

Spinal Muscular Atrophy (SMA) is a genetic disorder marked by progressive motor neuron loss in the spinal cord, resulting in muscle weakness and atrophy[1,2]. It is caused by mutations and deletion in the Survival Motor Neuron 1 (*SMN1*) gene, crucial for SMN protein production[3]. This protein deficit impairs the maintenance and function of motor neurons, culminating in their gradual deterioration and death. Therapies like Spinraza, Zolgensma, and Evrysdi, which increase SMN1 protein levels through gene replacement or SMN2 splicing modulation, have improved life expectancy and motor function, especially with early treatment[4,5,6,7]. The efficacy of these treatments declines once symptoms are advanced, highlighting the need for early intervention[7]. High costs and potential side effects further complicate these therapies, underscoring the need for more accessible and effective treatments.

A nearly identical copy of *SMN1*, *SMN2*, is normally expressed in all patients with SMA. Although a small amount of full-length protein that is identical to *SMN1* is produced, an exon-splicing silencer bearing a C-to-T transition in exon 7 of *SMN2* in all individuals skips exon 7[8,9]. We found that exon 7 deletion leads to reduce of *SMN* prion-like activity. The loss of a prion-like domain in SMA causes aberrant assembly of gemins and RNPs, misfolded protein aggregation of TDP-43 and PFN1, and neurodegeneration. Notably, these toxic misfolded proteins of TDP-43 and PFN1 remain after treatment with Spinraza and Evrysdi. Significantly, baicalein known as an off-amyloid stabilizer, endowed SMNΔ7 proteins, which is encoded by *SMN2*, to adopt a prion-like conformation, effectively restoring the cellular functions of SMN, eliminating toxic protein aggregates of TDP-43, and rescuing SMA in human dermal fibroblasts (HDFs) and a mouse model of SMA[10,11]. Our findings revealed an intrinsic molecular property of SMN, which is precisely linked to SMA, and offers us an opportunity to treat SMA patients with simply restoring prion-like activity.

Results

Formation of SMN Fibers in Hydrogels and Neuropathology Induced by SMN Prion-Like Deficiency

SMN1 has been shown to concentrate in subnuclear bodies called Gems which disassembled in SMA patients, and are incorporated into cytosolic stress granules (SG) through interaction with a prion-like protein, TIA1[12, 13]. We hypothesized that the SMN1 protein harbors prion-like low complexity (LC) domains. Indeed, when SMN1 recombinant proteins were assembled in vitro, they formed fibral structures in hydrogels, similar to the protein fibers with prion-like LC domains identified by Kato et al. (Fig. 1a, marked with arrowheads)[14]. The unstructured regions of SMN1 were mainly localized to amino acids 1-26, 61-87, 149-232 and 242-256 by IUPred2A prediction program (Fig. 1b). The analysis of low complexity regions (LCRs) in the SMN1 protein sequence, identified through SEG-based algorithms. The highlighted LCRs include serine-glycine (SG) rich regions at positions 3-10, lysine (K) rich regions at 64-87, glutamic acid-asparagine (EN) rich regions at 146-165, proline-glycine (PG) rich regions at 193-211, and proline (P) rich regions at 204-234 and 233-250. These regions, characterized by a high incidence of specific amino acids, suggest segments of the protein with reduced complexity.

Biotinylated isoxazole (b-isox), a specific chemical probe, selectively precipitates with proteins with prion-like low complexity (LC) domains, including TDP-43 and Fus[14,15]. We incubated 100 mM b-isox with SMN1 recombinant proteins and cell lysates of mes23.5 cells at 4°C to chemically precipitate prion-like proteins and then analyzed the presence of SMN1 by western blotting (Fig. 1c and d). Western blotting revealed the precipitation of both recombinant and cellular SMN proteins by b-isox (Fig. 1c and d). The major conformation of SMN recognized by b-isox was located in the cytosol (Fig. 1d). SET and PFN1 were used as fractionation controls. Notably, subcellular fractionation analysis further revealed that endogenous sumoylated SMN proteins were the predominant SMN conformations detected in insoluble urea fractions, and these proteins disappeared following b-isox treatments (Extended Data Fig. 1). Consistently, insoluble SMN has been reported to be important for the assembly of Cajal bodies (CBs) via the SUMO-like interacting motif (SIM-like)[16]. We speculated sumoylation is one of the cellular regulatory mechanisms that trigger nuclear SMN to form the separated phase though cross-b polymerization.

To locate the prion-like domain of SMN, we examined the capability of full-length SMN (SMN-FL) and a panel of exon-deleted SMN constructs to form gems, i.e., their liquid-liquid phase separation (LLPS) capability. A map of the SMN variants and the results are shown in Fig. 1g. Only fragments containing the region encoding exons 6-7 formed visible granules (Fig. 1g, arrowhead). The dynamics of mCherry-$SMN_{exon6-7}$ granules in living cells were further analyzed by time-lapse microscopy, and the trajectory of mCherry-$SMN_{exon6-7}$ granules is shown in Extended Data Fig. 2a. Most of the mCherry-$SMN_{exon6-7}$ granules traveled within a limited region, and two independent mCherry-$SMN_{exon6-7}$ granules occasionally underwent fission and fusion (Extended Data Fig. 2b, arrowheads). The average speed of mCherry-$SMN_{exon6-7}$ granules was ~0.8 μm/s. As the prion-like domain of SMN is located in exons 6-7, we inferred that the SMNΔ7 protein, which is encoded by *SMN2*, is an inactive prion-like SMN protein.

Unexpectedly, besides the regions containing exons 6-7, segments encoded by exons 1-3 were also found to precipitate with b-isox (Fig. 1h). This phenomenon is supported by consistent evidence of self-interactions within the domains of exons 2b and 6, indicative of prion-like cross-β interactions. Although both domains from exon 2 and exon 6 are potential capable of phase transitions through cross-β polymerization, only the fragments encompassing the region from exon 6 formed visible granules, as highlighted in Figure 1g (arrowhead). This indicates that additional elements are necessary for the development of membraneless compartments. Gemin2, used as a control, did not precipitate with b-isox.

Next, we assessed the prion-like properties of SMNΔ7 proteins encoded by SMN2. Our experiments showed that SMNΔ7 recombinant proteins can be precipitated with b-isox and subsequently form fibrous structures in hydrogels (Fig. 1.i and j). However, the SMNΔ7 fibers were approximately one-third shorter than those of full-length SMN, indicating a reduced prion-like propensity for SMNΔ7 (Fig. 1k). Considering potential changes in heterotypic interactions within the cross-β structures of prion-like LC domains, we explored the implications of reducing the prion-like characteristics of SMN in SMA, particularly focusing on its impact on other cellular prion-like proteins. We evaluated global changes in prion-like LC protein expression in SMA by analyzing spinal cord lysates from type I SMA-like mice and their control littermates. Using b-isox precipitation followed by LC-MS/MS identification, we isolated prion-like LC proteins. Differential b-isox-bound proteins were then examined using the DAVID Functional Annotation Bioinformatics Analysis (https://david.ncifcrf.gov/tools.jsp) database to identify enriched Gene Ontology (GO) terms. According to GO enrichment analysis (FDR-adjusted $P \leq 4.95E{-}5$, Fig. 1l), there was a decrease in the expression of b-isox-precipitated proteins involved in RNA binding and RNP assembly, underscoring the critical role of SMN in the prion-like assembly of RNPs. Aligning with GO analysis results, 15 of the 48 downregulated proteins were RNA-binding proteins (Fig. 1l). Figures 1m and 1n depict the prion-like proteins interactome of upregulation and downregulation in SMA. The interactome analysis revealed that RNP-related proteins constitute the most significantly upregulated category, while chromatin-related mechanisms represent the most significantly downregulated category (Fig. 1m and n).

Baicalein Endows SMNΔ7 with SMN-FL Prion-Like Functions and Achieves Precise Reversal of SMA Pathological Pathways

In our search for an activator to restore SMN cross-β interactions, we screened a chemical library and discovered that baicalein normalizes the assembly of gems in type III SMA patient-derived human dermal fibroblasts (HDFs) (Fig. 2a). Statistical analysis detailing baicalein's effect on gem formation is presented in Figure 2b. Importantly, we observed restoration of SMN proteins by baicalein in SMA patient-derived HDFs (Fig. 2c). As SMA patient-derived HDFs express only the SMNΔ7 protein, we speculated that baicalein restores the formation of gems in SMA patient-derived HDFs by altering the conformation of the nonfunctional prion-like C-terminus of SMNΔ7. We used the b-isox precipitation assay to assess the cross-β conformation of SMNΔ7 *in vivo* and found that the cross-β conformation of SMNΔ7 in baicalein-treated SMA patient-derived HDFs was the same as that of SMN-FL (Fig. 2d). These

results suggest that baicalein may endow the nonfunctional SMNΔ7 C-terminus with the ability to adopt a prion-like conformation.

We next assessed whether these SMNΔ7 proteins with baicalein-induced restoration of prion-like activity can perform the unique cellular functions of SMN1. We measured the length of axons of neurons transfected with SMNΔ7 in the presence or absence of baicalein, as neurons transfected with SMNΔ7 extend significantly shorter neurites than those transfected with SMN-FL[17]. Indeed, baicalein increased the length of axons from NSC34 cells expressing SMNΔ7 by approximately 2 fold (Fig. 2e); the results of statistical analysis are shown in Fig. 2f. Given that the protein half-life of SMNΔ7 is half as long as that of SMN-FL in cells, we investigated the stability of SMNΔ7 in the presence of baicalein. Our findings reveal that baicalein significantly enhances the stability of both recombinant and cellular SMNΔ7 proteins (Fig. 2g and h, arrow)[18]. Additionally, as PFN1 is known to effectively interact with SMN but not SMNΔ7, we analyzed the interactions of SMNΔ7 and PFN1 in baicalein-treated cells by coimmunoprecipitation (Fig. 2i)[19,20]. The results showed that in the presence of baicalein, the interaction between PFN1 and SMNΔ7 was significantly increased (Fig. 2i, arrowhead).

To identify baicalein's pharmacological targets in SMA, we collected protein lysates from NSC34 cells treated with and without baicalein, precipitated the proteins using b-isox, and identified them by LC–MS/MS. Differential protein expression was analyzed using the DAVID database to identify enriched GO terms. In baicalein-treated NSC34 cells, the top five upregulated GO terms, associated with Smn functions such as Sm core formation, SnRNP assembly, RNA binding, and RNA splicing (FDR adjusted P ≤ 1.09E-9, Fig. 2j), highlight its impact. Of the 71 proteins modulated by baicalein, 26 are directly linked to Smn or its complexes (Fig. 2j). Additionally, the interactome of upregulated proteins is depicted in Figure 2k, while the interactome of downregulated proteins, which are typically upregulated in SMA and related to chromatin mechanisms, is presented in Figure 1l-n. We found that baicalein precisely reverses the most critical aberrant cellular pathways in SMA. Together with the results in Figure 2, these findings suggest that baicalein endows SMN2 encoded SMNΔ7 with prion-like bioactivity, allowing it to behave similarly to SMN-FL.

Baicalein Effectively Improves Survival and Motor Neuron Functions in SMA Mice

To determine whether the *in vitro* findings could be recapitulated *in vivo*, we administered baicalein (13.6 mg/kg/d) or DMSO (control) to late-onset type III SMA model mice daily by intraperitoneal injection. After 4 weeks of treatment, histological analysis of lumbar spinal sections from SMA mice confirmed an increase in the ChAT-positive motor neuron number (Fig. 3a, P=0.0435) and recovery of nuclear gem formation (Fig. 3A, bottom, P=0.0063, labeled by arrowheads in Fig. 3a).

We found that SMN protein levels but not *SMN* mRNA levels were increased in various tissues from baicalein-treated SMA mice compared with those from control SMA mice (Fig. 3b) (Extended Data Fig. 3), confirming that baicalein increases the protein stability of SMND7, consistent with the data shown in Fig. 2G. Beginning at 7 months of age, we treated type III SMA mice with baicalein for four months,

which improved mouse survival (*P*=0.048) (Fig. 3c). A reduction in the evoked compound muscle action potential (CMAP) amplitude upon sciatic nerve stimulation was observed in control SMA mice (Fig. 3d, left, *P*=0.0201), but this phenomenon was abolished in baicalein-treated SMA mice (Fig. 3d, right, *P*=0.3326). Baicalein-treated SMA mice showed better motor performance than control mice in both the fixed-speed and accelerating rotarod tests, as determined by measuring the latency to fall (Fig. 3e and f). Fluorogold retrograde tracing of spinal motor neurons revealed a higher motor neuron density within the anterior horn (Fig. 3g, left, *P*=0.0114) and more large a-motor neurons (Fig. 3g, right, *P*=0.0037) in baicalein-treated mice than in control SMA mice. Significantly, baicalein treatment increased the axonal innervation of neuromuscular junctions (NMJs) in the hamstring muscles of SMA mice (Fig. 3h, *P*=0.04).

Next, we administered baicalein (13.6 mg/kg/d) or DMSO (control) to early-onset type I SMA model mice daily by intraperitoneal injection beginning at birth. We expected that the therapeutic efficacy of baicalein on type I SMA mice was weaker, as SMN2 protein levels are lower in type I SMA than in type III SMA. After baicalein treatment, the motor function of SMA mice, including the righting time, tube score, and tilting score, was improved on the 6th postnatal day (*P*<0.05), and the results were similar to those for heterozygous littermates treated with or without baicalein (Extended Data Fig. 3). On the 8th postnatal day, the motor function of baicalein-treated SMA mice was better than that of untreated SMA mice in the tube test (*P*=0.009) but not in the turnover test (*P*=0.065) or negative geotaxis test (*P*=0.58) (Extended Data Fig. 4). However, baicalein-treated type I SMA mice showed lifespans (8.8±0.4 vs. 7.9±0.2 days; *P*=0.13) and body weight gains that were similar to those of control SMA mice. The weaker effects of baicalein treatment on type I SMA mice than on type I SMA mice supports that baicalein targets to SMN2, endowing it with prion-like activity to perform the prion-like functions of *SMN1 in vivo*.

TDP-43 and PFN1 Aggregation in SMA Remains Unresolved by Current Therapeutic Drugs

We next conducted a detailed examination of prion-like interaction partners of SMN, including TDP-43 and PFN1, in SMA models. TDP-43, a molecule critically involved in ALS, often aggregates in approximately 80% of ALS patients[21]. Our studies show degraded TDP-43 proteins shift into an insoluble fraction, a process reversible by baicalein treatment (Fig. 4a). Immunofluorescence confirmed the presence of cytosolic TDP-43 aggregates in SMA patient-derived HDFs, which dispersed following baicalein treatment (Fig. 4b). Similar mislocalization and nuclear envelope deposition were observed in spinal cord motor neurons of SMA mice, indicated by arrowheads and arrows respectively in Figure 4c. These results suggest that a deficiency in one prion-like protein may disrupt the prion-like folding of its interaction partners, leading to aggregate formation. We have recently shown baicalein as a prion-like stablizer of TDP-43, restores TDP-43 cellular functions by correcting misfolded aggregates of TDP-43[11].

To further confirm this phenomenon, we analyzed another protein, PFN1. Previous studies have suggested that PFN1 regulates cytoskeletal dynamics through direct interactions with the polyproline stretch in SMN, located in the self-oligomerization region. PFN1 is known to misfold and form cytosolic aggregates in ALS patients[22]. In SMA patient-derived HDFs, immunofluorescence staining revealed that PFN1 also formed cytosolic aggregates (Fig. 4d). Interestingly, treatment of healthy HDFs with b-isox,

which interferes with physiological cross-β interactions of prion-like low-complexity (LC) proteins, significantly reduced the number of Gems while increasing misfolded PFN1 aggregates in a dose-dependent manner (Fig. 4e).

As SMA patient biopsies were inaccessible, we employed a b-isox based plasma test to detect misfolded TDP-43 and PFN1, previously validated their specificity and accuracy in ALS (Lai et al., revision; Ting et al., reviewing). We observed elevated plasma levels of TDP-43 in SMA patients compared to healthy individuals, which returned to normal after depletion with anti-amyloid oligomer antibody A11, suggesting the presence of toxic TDP-43 oligomers in SMA patients (Figs. 4f-g)[23]. Similarly, elevated PFN1 levels returned to normal after preabsorbing amyloid oligomers with the A11 antibody. These results suggested the presence of misfolded TDP-43 and PFN1 proteins in SMA patients (Figs. 4h-i). Plasma levels of ANX5 and SOD1, which are altered in ALS, remained unchanged in SMA (Extended Data Fig. 5).

Lastly, we monitored the plasma levels of misfolded TDP-43 and PFN1 in response to treatments with ASO (Spinraza) or Risdiplam (Evrysdi), which are known to increase SMN proteins. Unfortunately, we did not observe significant reductions in plasma levels of TDP-43 or PFN1 oligomers after treating with Spinraza or Evrysdi (Figs. 4j-k). We hypothesize that the persistent presence of toxic misfolded proteins due to unresolved SMN1 prion-like deficits may underlie the poor drug efficacy observed in adult SMA patients. These findings obtained from figure 4, suggest a potential common etiology shared between SMA and ALS.

Discussion

The deficiency of SMN protein is widely recognized as the pathological basis of SMA. Current therapeutic interventions primarily focus on modifying the RNA splicing of the SMN2 gene to increase the levels of functional SMN1 protein. However, these therapies are not only costly but also exhibit limited efficacy. It is important to note that the full-length SMN protein possesses two prion-like domains. Proteins with prion-like domains are prone to forming aggregates within the cell. This propensity can influence the aggregation behavior of other prion-like proteins, creating a cascade of protein misfolding events that can lead to cell death and disease progression. In the context of SMA, the absence of sufficient SMN1 protein facilitates the misfolded aggregation of other prion-like proteins, such as TDP-43. These misfolded aggregates contributes to the disease's pathophysiology, categorizing SMA as a conformational disease. Therefore, an effective therapeutic approach for SMA should not solely focus on restoring SMN protein levels but must also address the aggregation of TDP-43 and other prion-like proteins. This dual approach could potentially explain the limited success of current therapies that only target SMN protein restoration.

We identified a small compound named baicalein, which addresses prion-like propensity deficiencies by enabling the prion-like structure of SMNΔ7 and dissolving protein aggregates of TDP-43 and PFN1, acting as an off-amyloid stabilizer. Unlike current therapies that primarily increase SMN protein levels,

baicalein not only restores the SMN complex and Gemins, but also disassembles aggregated proteins and effectively mitigating the pathological consequences of SMN prion-like deficiency. Notably, its precise targeting of prion-like SMN-deficient pathways in SMNΔ7 and TDP-43 proteins ensures rapid therapeutic effects without off-target impacts (Fig. 5). Finally, baicalein is affordable compared to the extremely high costs of existing SMA treatments, making it a promising and cost-effective therapeutic strategy.

Materials And Methods

Cell Culture and Drug Treatment

Human dermal fibroblasts (HDFs) were cultured in medium 106 (Gibco®, Thermo Fisher Scientific) with low serum growth supplement (LSGS) (Gibco®, Thermo Fisher Scientific) and 1% penicillin-streptomycin (Gibco®, Thermo Fisher Scientific) as previously described[19]. To determine the effects of compounds on the LLPS of prion-like proteins, the cells were treated with baicalein or b-isox for 24 or 48 h at the indicated concentrations (5, 10, 25, or 50 μM). Transfections were performed using Lipofectamine^{TM} 2000 or Lipofectamine^{TM} 3000 (Thermo Fisher Scientific) according to the manufacturer's protocol. Briefly, cells were seeded into the wells of a 96-well plate ($7.5´10^3$ cells for viability assays), a 12-well plate ($1.5´10^5$ for immunocytochemistry (ICC) studies) or a 6-well plate ($5´10^5$ for time-lapse studies) and cultured overnight. Cells transfected with mCherry-SMND7 expression plasmids were assayed for neurite outgrowth at 48 h posttransfection. Baicalein (50 mM) was added at 24 h posttransfection, and neurite outgrowth was determined 24 h after drug addition.

Patient Eligibility

Participants included SMA patients and similar-aged healthy from National Taiwan University Hospital, Taipei. Plasma from SMA patients with survival motor neuron 1 gene mutations (average age 40.6, 38% women) was collected. The study was approved by the National Taiwan University Hospital's Research Ethics Committee (202303106RINB).

Reagents and Antibodies

b-isox, obtained from Sigma and Dalton, was dissolved in dimethyl sulfoxide (DMSO). A11 (Anti-Amyloid Oligomer Antibody, αβ, oligomeric, AB9234) were purchased from Merck Millipore. SMN and SMND7 recombinant proteins were acquired from OriGene. Hydrogel experiments were conducted according to Kato's protocol[14].

Subcellular Fractionation and Western blotting

Cultured 293T and mes23.5 cells were harvested using a subcellular protein fractionation kit (Thermo Fisher Scientific) according to the manufacturer's recommendations. Cell lysates were separated into five different cellular compartments. The fractionated proteins were used for Western blotting, as

previously described. The SMN and mCherry antibodies were kind gifts from Hung-Li. The profilin1 antibody was purchased from Proteintech (11680-1-AP).

b-isox Precipitation

Briefly, 293T cells were harvested and lysed with RIPA buffer. The protein concentration was adjusted to 1 to 10 mg/mL, and 10 mM b-isox was added to the cell lysate at a final concentration of 100 to 200 mM. The mixtures were then incubated at 4°C for 60 min and centrifuged at 15000 rpm for 15 min at 4°C, and the supernatant was discarded. All of the mixtures were subjected to SDS-PAGE and Western blotting.

Mice

A mouse model of SMA was produced by deleting exon 7 of the *Smn* gene and knocking in the human *SMN2* gene ($Smn^{-/-}SMN2^{+/-}$). We were able to generate a variant that exhibited more severe disease symptomatology by backcrossing to obtain a more homogenous genetic background with two copies of the *SMN2* transgene ($Smn^{-/-}SMN2^{+/-}$) (severe SMA model). We also generated a model of mild SMA, which carried four copies of the *SMN2* transgene ($Smn^{-/-}SMN2^{+/+}$). Both severe and mild SMA mice received daily intraperitoneal injections of baicalein (13.6 mg/kg/d in DMSO) or DMSO alone (control) from birth until death (severe SMA mice) or from 7 to 11 months of age (mild SMA mice). The severe SMA mice were then subjected to motor function tests and survival analysis. Mild SMA mice were subjected to motor function tests, survival analysis, electrophysiological studies, and pathological studies. Another group of mild SMA mice received the same dose of baicalein or DMSO at 4 months old for 2 weeks for Western blot and quantitative PCR analyses. Housing and husbandry were maintained with standard procedures in the NTUCM Laboratory Animal Center. All animal procedures in this study were approved by the Institutional Animal Care and Use Committee (protocol #20190314).

Motor Function Tests

For mild SMA mice, both fixed-speed (20 rpm for 5 min) and accelerating (from 4-40 rpm in 5 min) rotarod test protocols were conducted to evaluate motor function every 2 weeks, as previously described[24]. Mice were placed in a neutral position on the stationary 3-cm diameter cylinder of the rotarod apparatus (Singa RT-01), and the time to fall was recorded when each mouse fell off the rod. For severe SMA mice, the turnover, tube and negative geotaxis tests were conducted at 6 and 8 days old, as previously described[25]. In the turnover test, the time required for a mouse to right itself and place all four paws on the ground from a prone position was recorded (the cutoff time was 60 sec). The tube test was used to determine hind limb strength according to the posture of the hind limbs and the tail; scores ranged from 0 (the worst) to 4 (the best). In the negative geotaxis test, mice were placed on a 45° incline with their head pointing downward. The responses (turning and climbing) were scored from 0 (worst) to 4 (best).

Retrograde Tracing, Immunocytochemistry, and Immunohistochemistry

For retrograde motor neuron tracing, fluorogold dye (Fluorochrome, LLC) was injected into the bilateral gastrocnemius and tibialis anterior muscles of mild SMA mice (2 µL for each muscle) 3 days before sacrifice. For immunocytochemistry, HDFs were fixed and blocked as previously described[24]. Gem number counts and SMN nuclear localization in fibroblasts were confirmed using DAPI counterstain. For immunohistochemistry, lumbar spinal cords and hamstring muscles from mild SMA mice were fixed with 4% paraformaldehyde (PFA) and dehydrated in a series of sucrose solutions. Lumbar spinal cord cryosections (10 µm) and hamstring muscle cryosections (15 mm) were blocked, permeabilized, and incubated with the appropriate antibodies as previously described[29, 30]. Images were obtained using a Zeiss LSM880 microscope (Carl Zeiss) with a 10´ or 20´ objective lens (plan-apochromat 20´/0.8 M27 and plan-apochromat 40´/1.3, oil, DIC M27). The mean number of motor neurons per anterior horn, nuclear gem counts per motor neuron, and percentage of axonal innervation at the NMJ were calculated for each animal. The primary antibodies included anti-SMN, anti-ChAT (EMD Millipore, #AB144P), anti-neurofilament-H 200 kDa (EMD Millipore, #AB1989), anti-synaptophysin (Abcam, #ab32127), and α-bungarotoxin Alexa Fluor 555 conjugate (Thermo Fisher Scientific, #B35451).

Electrophysiological Study

The mice were anesthetized with Zoletil (20 mg/kg, ip). The skin in the right hind limb was shaved and adorned with surface nonpolarizable Ag/AgCl electrodes (Ambu^{Ò} Blue Sensor NF, Ambu A/S, Denmark), which were trimmed to approximately 0.5cm ´ 0.5cm over the gastrocnemius muscle. An invasive needle electrode was placed near the sciatic notch for stimulation, and the ground was placed on the tail with an invasive needle electrode. The recording was performed with a Nicolet EDX System and Synergy interface (Natus Medical Incorporated, USA). The stimulation was increased gradually to obtain supramaximal stimulation and a stable CMAP amplitude.

Time-lapse Study

Briefly, 293T cells were first seeded on glass slides in 6-well culture plates and then transfected with mCherry-tagged plasmids. After 48 h, a glass slide was placed into a perfusion, open, and closed (POC) chamber (Pecon) and into an incubator containing a spinning disk confocal microscope (Axio-observer. Z1/7, Zesis). Images were acquired under a 63´ objective lens (plan-apochromat 63´/1.40, oil, DIC, M27) using the mCherry (EX 572/35, EM 632/60) filter set for 2 min at appropriate time intervals. Analysis was conducted using the integrated ZEN (v.3.1) imaging program and Imaris software (v.9.6.0, Bitplane).

b-isox-based Enzyme-Linked Immunosorbent Assay (ELISA) and Depletion of Amyloid oligomers

Blood samples from patients and healthy controls were collected using Blood Collection Tubes, centrifuged at 2,200 × g for 15 minutes to separate plasma. For the immunoassay, 50-100 µL of plasma was mixed with 0.5-1 µL of b-isox, and rotated for 1 hour at 4°C. Streptavidin-coated microwells were washed thrice with 200 µL of wash buffer (WB) and filled with 100 µL of the reaction mixture, then incubated for 2 hours with shaking at room temperature (RT). Following three WB washes, wells were incubated with 100 µL of diluted primary antibody (1:500 in WB) for 1 hour with shaking at RT. After three

more WB washes, 100 µL of HRP-conjugated secondary antibody (1:15,000 in WB) was added, and wells were incubated for another hour with shaking at RT. Post-wash, 100 µL of TMB Substrate Solution was added to each well, incubated for 15-30 minutes until color development, and stopped with 100 µL of 2M sulfuric acid. Optical density at 450 nm was measured using a microplate reader. For depletion of amyloid oligomers, human plasma samples (50 µL) were incubated with A11 antibody overnight at 4°C with rotation. The next day, they were mixed with 5 µL of protein A/G magnetic beads (ThermoFisher) for 1 hour at room temperature with rotation. After magnetic separation for 3 minutes, the supernatants were collected for b-isox ELISA analysis with specific biomarkers.

Declarations

Acknowledgments

We thank the staff at the Image Core at Academia Sinica and the Core Labs at the Department of Medical Research, National Taiwan University Hospital for their assistance with the confocal microscopy and technical support. The SMN constructs were kindly gifted by Dr. Li-Hung at IMB, Academia Sinica. We dedicate this work to Dr. Hung-Li and commemorate and thank him for inspiring our academic careers. This research was funded by Garage Brain Science (ND-002), YEEFAN Med Inc. (SMA-01), and was supported by the Ministry of Science and Technology in Taiwan to Dr. L.-K. Tsai (108-2314-B-002-082-MY3).

Authors' Contributions

H.-Y. Chang and I.-F. Wang characterized the prion-like properties of SMN1 and its mutants. C.-H. Ting analyzed axonal outgrowth and gem bodies in patient-derived HDFs and performed time-lapse recording. C.-H. Ting, H.-J. Lai, C.-L. Chen and L.-K. Tsai performed the pharmacological analysis of baicalein in SMA mice. G.-G. Liou and J.-J. Liou performed EM study. C.-H. Ting, L.-K. Tsai, H.-Y. Chang, J.-J. Liou and I.-F. Wang wrote the manuscript, which was approved by all coauthors.

Conflict of Interest Statement

H.-Y. Chang, C.-H. Ting and I.-F Wang are financially compensated as employees of Garage Brain Science Co., Ltd. in Taiwan and YEEFAN MED INC. in the US.

References

1. Brzustowicz, L. M. et al. Genetic mapping of chronic childhood-onset spinal muscular atrophy to chromosome 5q11.2-13.3. *Nature* **344**, 540-541 (1990).
2. Melki, J. et al. Gene for chronic proximal spinal muscular atrophies maps to chromosome 5q. *Nature* **344**, 767-768 (1990).
3. Lefebvre, S. et al. Identification and characterization of a spinal muscular atrophy-determining gene. *Cell* **80**, 155-165 (1995).

4. Cartegni L., & Krainer A.R. Correction of disease-associated exon skipping by synthetic exon-specific activators. *Nat. Struct. Biol.***10**,120–125 (2003).
5. Valori, C. F., Ning, .K, & Wyles, M. et al. Systemic delivery of scAAV9 expressing SMN prolongs survival in a model of spinal muscular atrophy. *Sci Transl Med***2**, 35ra42 (2010).
6. Naryshkin, N. A. et al. Motor neuron disease. SMN2 splicing modifiers improve motor function and longevity in mice with spinal muscular atrophy. *Science.***345**, 688-693 (2014).
7. Timing is everything: Clinical evidence supports pre-symptomatic treatment for spinal muscular atrophy. *Cell Report Medicine*. 3, 100725 (2022).
8. U. R. Monani, C. L. Lorson, D. W. Parsons, T. W. Prior, E. J. Androphy, A. H. Burghes, J. D. McPherson, A single nucleotide difference that alters splicing patterns distinguishes the SMA gene SMN1 from the copy gene SMN2. *Hum. Mol. Genet.* **8**, 1177–1183 (1999).
9. Le, T. T. et al. SMNDelta7, the major product of the centromeric survival motor neuron (SMN2) gene, extends survival in mice with spinal muscular atrophy and associates with full-length SMN. *Hum. Mol. Genet.***14**, 845-857 (2005).
10. Wang, I. F.et al. The self-interaction of native TDP-43 C terminus inhibits its degradation and contributes to early proteinopathies. *Nat Commun***3**, 766 (2012).
11. Chang, H. Y., & Wang, I. F. Restoring functional TDP-43 oligomers in ALS and laminopathic cellular models through baicalein-induced reconfiguration of TDP-43 aggregates. *Sci Rep.***14**, 4620 (2024).
12. Shpargel, K. B., & Matera, A. G. Gemin proteins are required for efficient assembly of Sm-class ribonucleoproteins. *Proc Natl Acad Sci U S A.* **102**, 17372-17377 (2005).
13. Hua, Y., & Zhou, J. Survival motor neuron protein facilitates assembly of stress granules. *FEBS Lett.* **572**, 69-74 (2004).
14. Kato, M. et al. Cell-free formation of RNA granules: low complexity sequence domains form dynamic fibers within hydrogels. *Cell***149**, 753-767 (2012).
15. Kwon, I. et al. Phosphorylation-regulated binding of RNA polymerase II to fibrous polymers of low-complexity domains. *Cell***155**, 1049-1060 (2013).
16. Riboldi, G. M. et al. Sumoylation regulates the assembly and activity of the SMN complex. *Nat Commun.***12**, 5040 (2021).
17. H. L. Zhang, F. Pan, D. Hong, S. M. Shenoy, R. H. Singer, G. J. Bassell, Active transport of the survival motor neuron protein and the role of exon-7 in cytoplasmic localization. *J. Neurosci.***23**, 6627-6637 (2003).
18. Burnett, B. G. et al. Regulation of SMN protein stability. *Mol. Cell. Biol.***29**, 1107–1115 (2009).
19. Giesemann, T. et al. A role for polyproline motifs in the spinal muscular atrophy protein SMN. Profilins bind to and colocalize with smn in nuclear gems. *J. Biol. Chem.***274**, 37908-37914 (1999).
20. Sharma, A. et al. A role for complexes of survival of motor neurons (SMN) protein with gemins and profilin in neurite-like cytoplasmic extensions of cultured nerve cells. *Exp. Cell Res*. **309**, 185-197 (2005).

21. Ling SC, Polymenidou M, Cleveland DW. Converging mechanisms in ALS and FTD: disrupted RNA and protein homeostasis. Neuron. 2013 Aug 7;79(3):416-38.
22. Wu, C. H. et al. Mutations in the profilin 1 gene cause familial amyotrophic lateral sclerosis. *Nature***488**, 499-503 (2012).
23. Kayed, R. et al. Fibril specific, conformation dependent antibodies recognize a generic epitope common to amyloid fibrils and fibrillar oligomers that is absent in prefibrillar oligomers. *Mol Neurodegener* **2**, 18 (2007).
24. Hsieh-Li, H. M. et al. A mouse model for spinal muscular atrophy. *Nat. Genet.***24**, 66-70 (2000).
25. Liu, H. C. et al. Sodium vanadate combined with l-ascorbic acid delays disease progression, enhances motor performance, and ameliorates muscle atrophy and weakness in mice with spinal muscular atrophy. *BMC Med.***11**, 38 (2013).

Figures

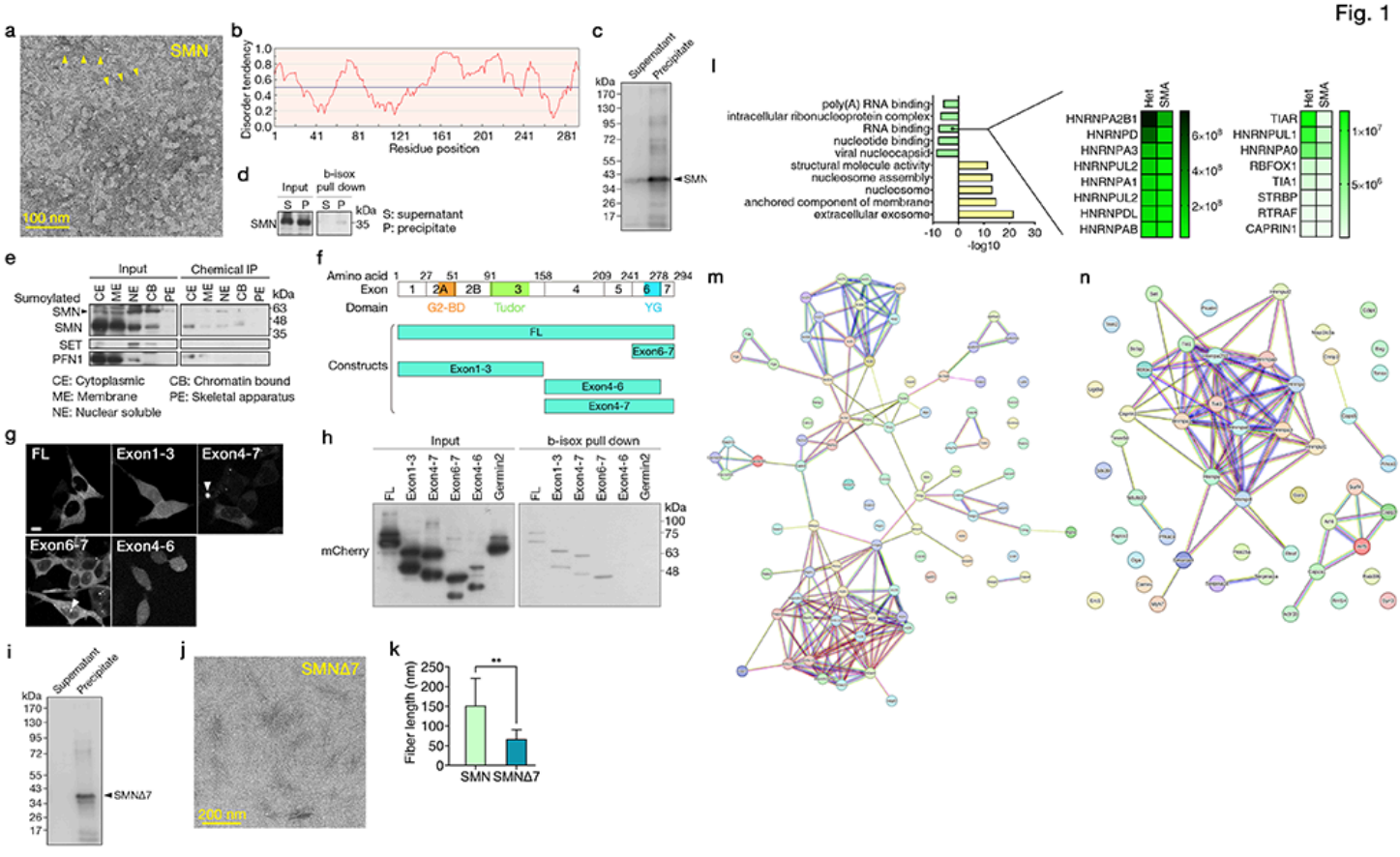

Figure 1

Characterization of SMN Prion-Like Domain and Its Neuropathology in Deficiency States. a, *In vitro* formation of SMN fibers. Scale bars: 100 μm. **b**, The IUPred prediction of intrinsically unstructured

regions of SMN. **c**, b-isox precipitates SMN recombinant proteins. **d**, b-isox precipitates SMN proteins from mes23.5 cells. **e**, Analysis of the levels of the prion-like conformers of SMN and PFN1 in different subcellular fractions of 293T cells. **f**, Schematics of SMN mutants. **g**, Subcellular localization of SMN variants. Scale bar, 10 μm. **h**, Identification of prion-like domain of SMN with b-isox. **i**, b-isox precipitates SMND7 recombinant proteins. **j**, *In vitro* formation of SMND7 fibers. Scale bars: 200 μm. **k**, Statistical analysis of the length of SMN and SMND7 fibers. ** $P < 0.01$ by t test. **l,** Proteome profiling of spinal cord samples from SMA mice reveals differentially expressed proteins bound by b-isox. Gene Ontology (GO) terms are enriched in upregulated (yellow) and downregulated (green) proteins. A heatmap illustrates the levels of downregulated RNA-binding proteins in the spinal cords of SMA mice, in comparison to heterozygous control littermates (Het). **m**, PPI network of upregulated proteins. **n**, PPI network of downregulated proteins.

Fig. 2

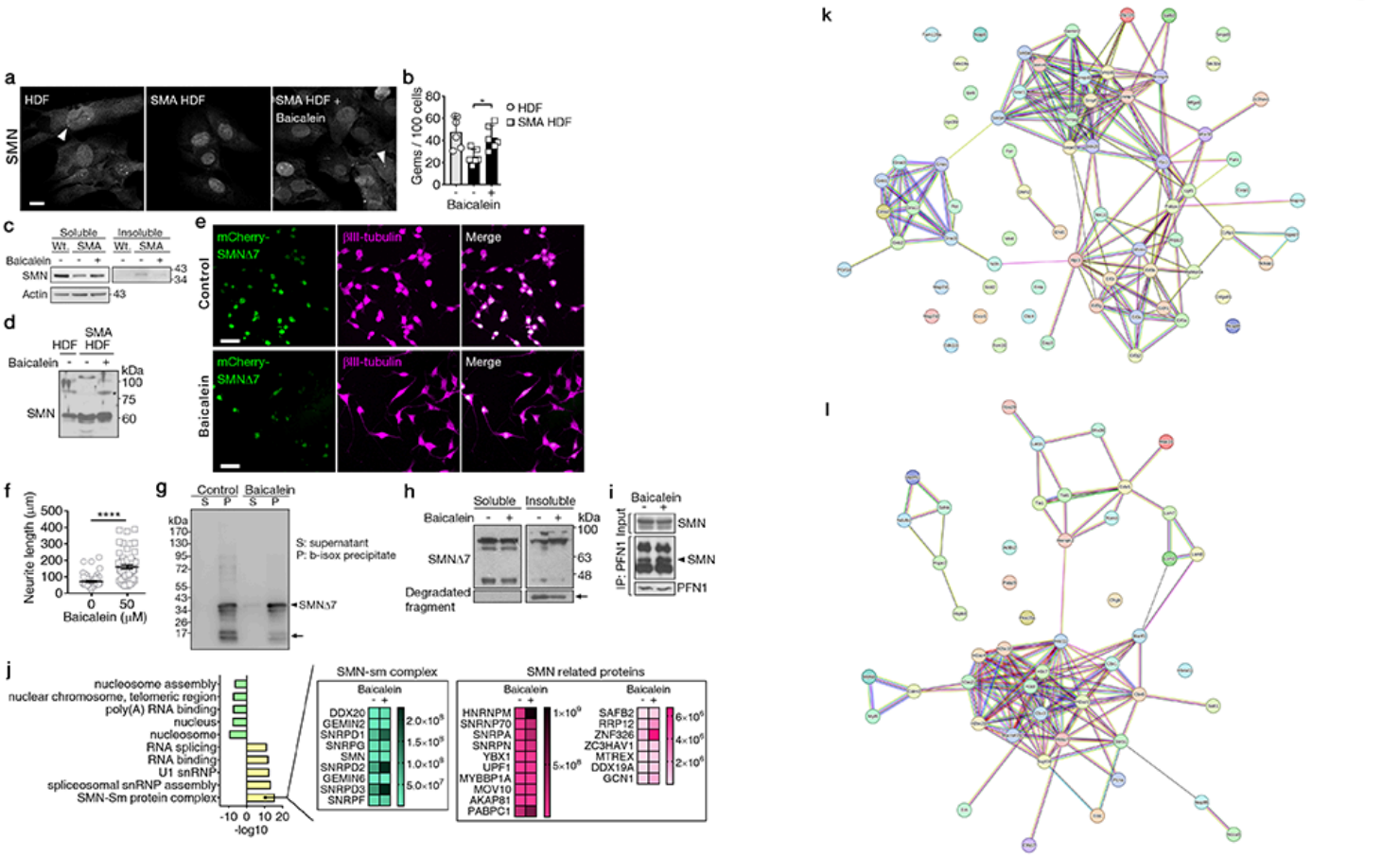

Figure 2

Mechanism underlying the effects of baicalein on SMN. a, Immunofluorescence images of gems in healthy control- and SMA patient-derived HDFs treated with or without baicalein. The arrowheads indicate gem bodies. Scale bars: 20 μm. **b**, Statistical analysis of gem numbers in healthy control- and SMA patient-derived HDFs treated with or without baicalein. All the data are presented as the mean and standard deviation (SD) (n= 6). * $P < 0.05$ by t test. **c**, Western blot analysis of SMN levels in HDFs derived from healthy controls and SMA patients treated with or without baicalein. **d**, Western blotting analysis of

SMN conformation in healthy control- and SMA patient-derived HDFs treated with or without baicalein. * indicates the baicalein-corrected structure of SMND7. **e**, Effects of baicalein on the axon length of cultured NSC34 motor neurons. Baicalein (50 mM)- or mock-treated NSC34 cells were stained with an anti-bIII-tubulin antibody (purple). SMND7-transfected cells express red mCherry. Scale bar, 50 μm. **f**, Statistical analysis of the neurite length of SMND7-transfected NSC34 cells treated with or without baicalein. ****P < 0.0001 by t test. **g**, Baicalein attenuated the degradation of the SMND7 protein. **h**, Baicalein attenuated the degradation of the SMND7 recombinant proteins. **i**, The physical interaction of SMND7 with PFN1 was examined in the presence of baicalein. **j,** Proteome profiling of b-isox bounded proteins in NSC34 cells with and without baicalein treatment. Gene Ontology (GO) terms for differentially expressed proteins are highlighted, with upregulated proteins associated with yellow GO terms and downregulated proteins with green GO terms. The heatmap details the levels of upregulated Smn-associated proteins in baicalein-treated cells (T) compared to mock-treated cells (Co). **k**, PPI network of upregulated proteins. **l**, PPI network of downregulated proteins.

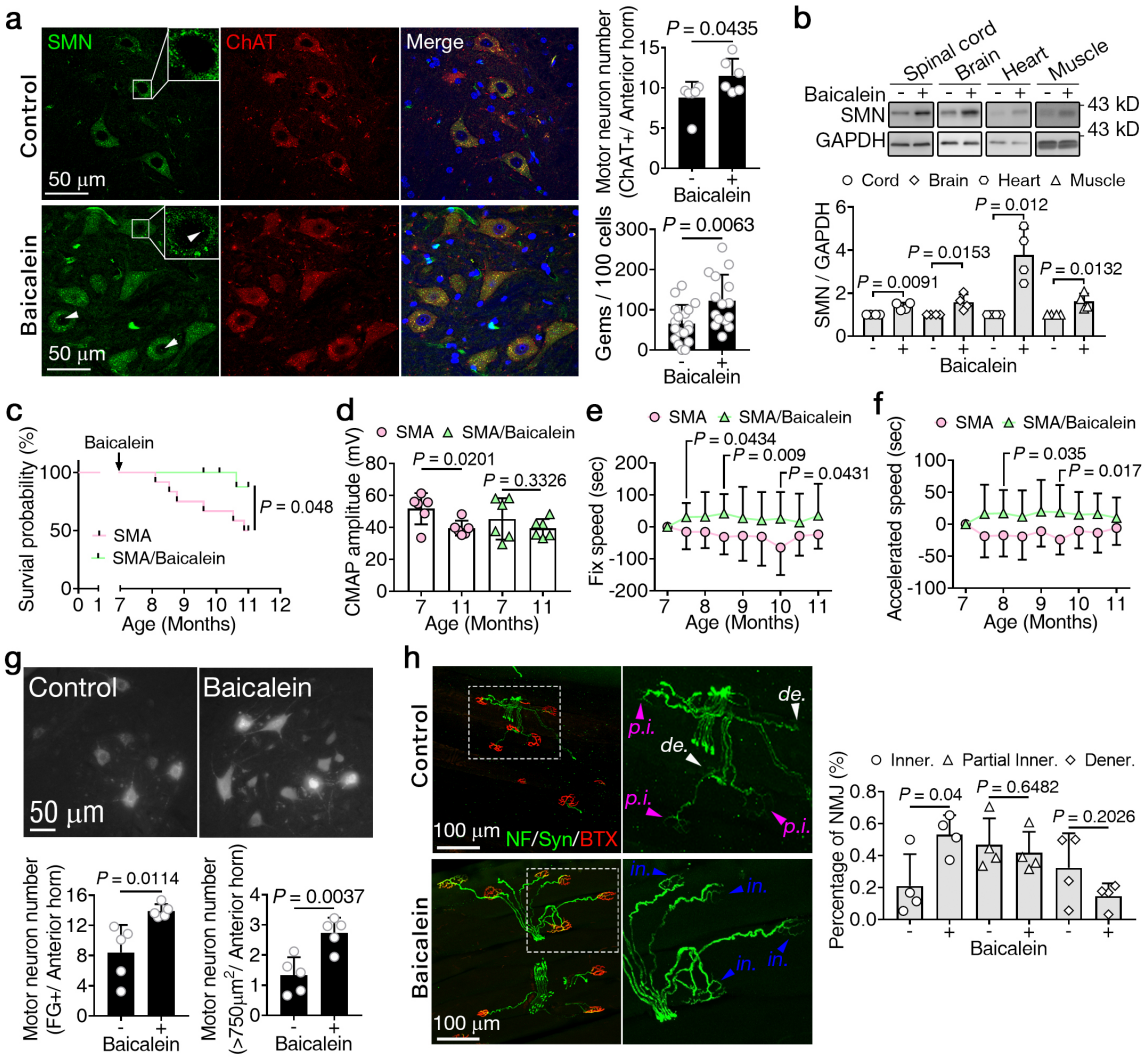

Figure 3

The treatments of SMA mice with baicalein, a, Histological staining of lumbar spinal motor neurons in SMA mice with or without baicalein treatment using anti-ChAT (red), anti-SMN (green), and DAPI (blue). The magnified region is shown in boxes to the right of the SMN panel, where the arrowheads show nuclear gems. Bar: 50 mm. Right, quantifications of ChAT-positive motor neuron and nuclear gem counts (per cell) in the anterior horn of SMA mice; *n* = 6 in each group. **b,** Western blot analysis of the Smn

expression in various tissues of SMA mice treated with or without baicalein daily for 2 weeks. Quantitation of the Smn expression relative to GAPDH as shown in the bottom; *n* = 4 in each group. **c,** Survival analysis of SMA mice treated with (*n* = 10) or without (*n* = 12) baicalein daily for four months beginning at 7 months of age. **d,** Comparison of compound motor action potential (CMAP) amplitudes between results at 7 (baseline) and 11 months of age in SMA mice with or without baicalein treatment; *n=6* in each group. **e-f,** Latency to fall from the fixed-speed (**h**) and accelerating (**i**) rotarod tests in baicalein-treated (*n* = 10) and control (*n* = 12) SMA mice. The values presented were normalized to the baseline data. **g,** Retrograde tracing of lumbar spinal motor neurons using intramuscular injection of fluorogold (FG) in SMA mice treated with or without baicalein for 4 months. Bottom, quantifications of the FG-positive motor neuron and large a-motor neuron (area > 750 mm^2) counts. Bar, 50 μm; *n* = 5 in each group. **h,** Staining with neurofilament-H/synaptophysin (green) and a-bungarotoxin (BTX) (red) reveals neuromuscular junctions (NMJs) in SMA mice. Bar: 100 mm. The magnified region is shown on the right, demonstrating nerve innervation (in.), partial innervation (p.i.), or denervation (de.) of NMJs. Right, quantification of NMJ patterns; *n* = 4 in each group. **b, d, g, h,** Unpaired two-tailed Student's *t*-test. **c,** Gehan-Breslow-Wilcoxon test. **e, f,** multiple *t*-test. The data are shown as the means ± SD, and *P* values < 0.05 were considered significant. **i**, Modeling of the prion-like conformation-based therapies for treating SMA with baicalein.

Fig. 4

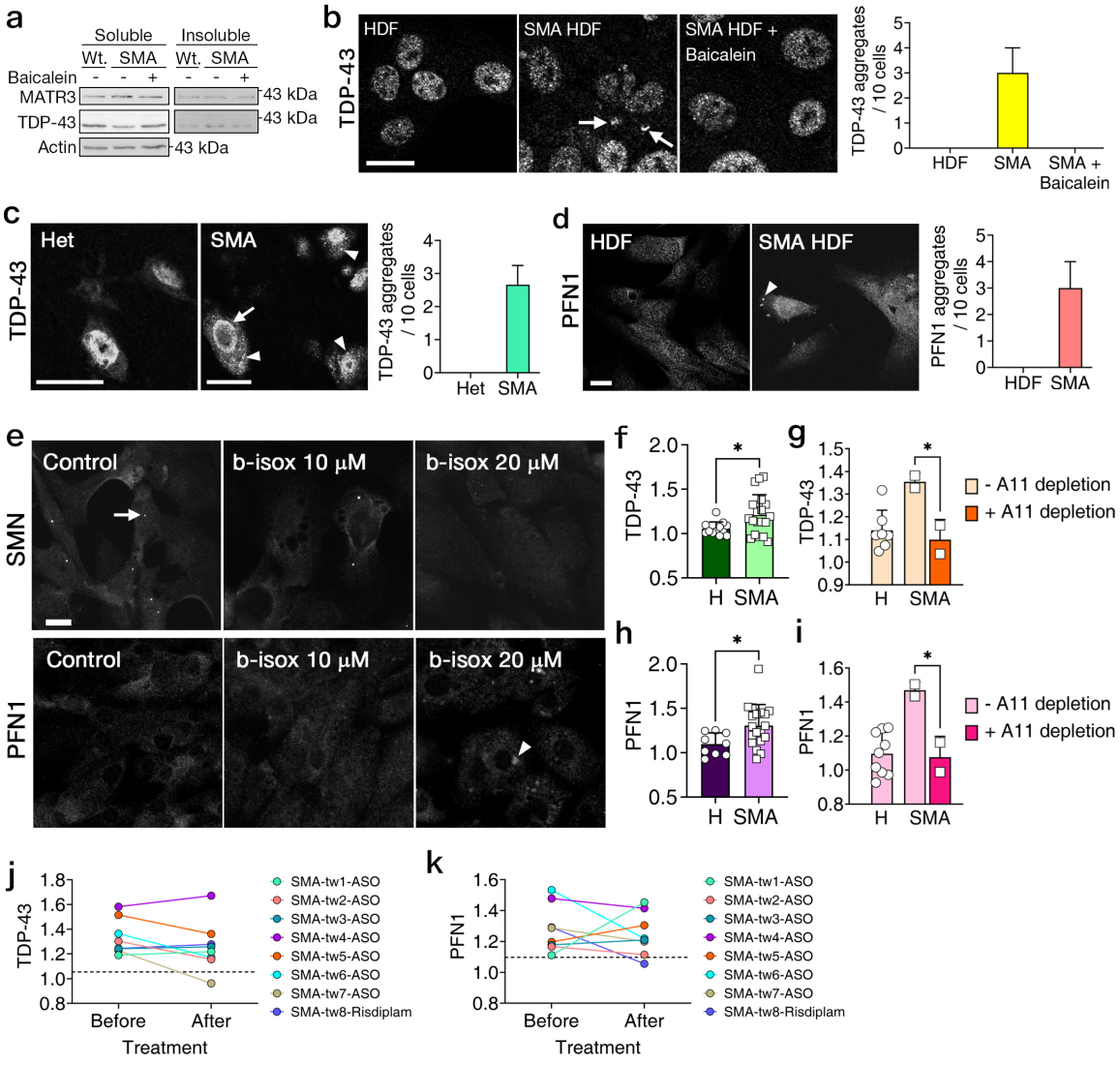

Figure 4

Assessment of TDP-43 and PFN1 in SMA Patients and Models and the Impact of Therapeutic Intervention. a, Western blot analysis of TDP-43 levels in HDFs derived from healthy controls and SMA patients treated with or without baicalein. **b**, Immunofluorescence images of TDP-43 in HDFs derived from healthy controls and SMA patients treated with or without baicalein. The arrows indicate TDP-43 aggregates. Scale bars: 20 µm. Statistical analysis of TDP-43 aggregate-positive cell percentage is

shown on the right. **c**, Immunofluorescence staining of TDP-43 in heterozygous control and SMA mice. Scale bars: 20 μm. Statistical analysis of TDP-43 aggregate-positive cell percentage is shown on the right. **d**, Immunofluorescence staining of PFN1 in healthy control- and ALS patient-derived HDFs. Scale bars: 10 μm. Statistical analysis of PFN1 aggregate-positive cell percentage is shown on the right. **e**, Immunofluorescence staining of SMN and PFN1 in healthy control-derived HDFs treated with 0, 10 or 20 μM b-isox. Scale bars: 20 μm. **f**, b-isox ELISA shows the plasma levels of TDP-43 in healthy individuals (H) and patients with SMA. All the data are presented as the mean and SD (n of H and SMA= 12 and 19, respectively.). *P < 0.05 by the Mann-Whitney test. **g**, A11 antibody abolished elevated levels of b-isox-captured TDP-43 in the plasma of SMA patients. *P < 0.05 by the ANOVA test. **h**, b-isox ELISA shows the plasma levels of PFN1 in healthy individuals (H) and patients with SMA. All the data are presented as the mean and SD (n of H and SMA= 9 and 19, respectively.). *P < 0.05 by the Mann-Whitney test. **i**, A11 antibody abolished elevated levels of b-isox-captured PFN1 in the plasma of SMA patients. *P < 0.05 by the ANOVA test. **j**, Comparative analysis of plasma misfolded TDP-43 in SMA patients treated with ASO (Spinraza) or Risdiplam (Evrysdi) Versus untreated patients. **k**, Comparative analysis of plasma misfolded PFN1 in SMA patients treated with ASO or Risdiplam Versus untreated patients.

Fig. 5

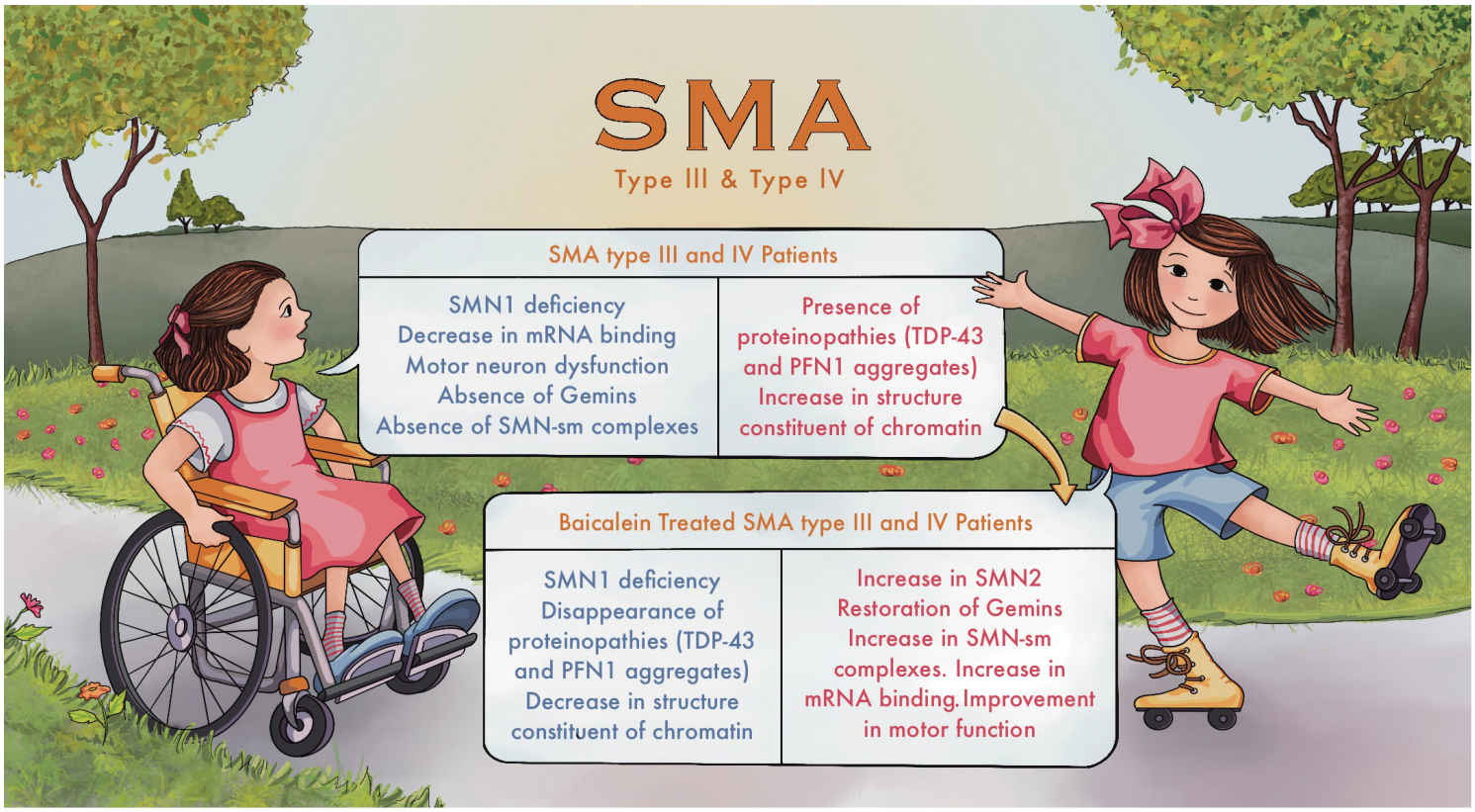

Figure 5

A Model of Baicalein's Dual-Action Mechanism in Treating SMA. Figure 5 illustrates baicalein's effectiveness in accurately reversing the pathologies associated with SMN prion-like deficiency, including restoration of gemins, mRNA binding, and SMN-sm complexes in SMA. Additionally, baicalein is effective in clearing misfolded proteins, tackling specific pathological features inadequately addressed by existing therapies.

Supplementary Files

This is a list of supplementary files associated with this preprint. Click to download.

- FigS1.3.jpg
- FigS2.2.jpg
- FigS3.2.jpg
- FigS4.1.jpg
- FigS5.jpg
- Wangsupplemental.docx